

# Systematic study of trace radioactive impurities in candidate construction materials for EXO-200

D.S. Leonard<sup>a</sup>, P. Grinberg<sup>b</sup>, P. Weber<sup>c,1</sup>, E. Baussan<sup>c,2</sup>,  
 Z. Djurcic<sup>a,3</sup>, G. Keefer<sup>a</sup>, A. Piepke<sup>a</sup>, A. Pocar<sup>d</sup>,  
 J.-L. Vuilleumier<sup>c</sup>, J.-M. Vuilleumier<sup>c</sup>, D. Akimov<sup>e</sup>,  
 A. Bellerive<sup>f</sup>, M. Bowcock<sup>f</sup>, M. Breidenbach<sup>g</sup>, A. Burenkov<sup>e</sup>,  
 R. Conley<sup>g</sup>, W. Craddock<sup>g</sup>, M. Danilov<sup>e</sup>, R. DeVoe<sup>d</sup>,  
 M. Dixit<sup>f</sup>, A. Dolgolenko<sup>e</sup>, I. Ekchtout<sup>f</sup>, W. Fairbank Jr.<sup>h</sup>,  
 J. Farine<sup>i</sup>, P. Fierlinger<sup>d</sup>, B. Flatt<sup>d</sup>, G. Gratta<sup>d</sup>, M. Green<sup>d</sup>,  
 C. Hall<sup>j</sup>, K. Hall<sup>h</sup>, D. Hallman<sup>i</sup>, C. Hargrove<sup>f</sup>, R. Herbst<sup>g</sup>,  
 J. Hodgson<sup>g</sup>, S. Jeng<sup>h</sup>, S. Kolkowitz<sup>d</sup>, A. Kovalenko<sup>e</sup>,  
 D. Kovalenko<sup>e</sup>, F. LePort<sup>d</sup>, D. Mackay<sup>g</sup>, M. Moe<sup>k</sup>,  
 M. Montero Díez<sup>d</sup>, R. Neilson<sup>d</sup>, A. Odian<sup>g</sup>, K. O'Sullivan<sup>d</sup>,  
 L. Ounalli<sup>c</sup>, C.Y. Prescott<sup>g</sup>, P.C. Rowson<sup>g</sup>, D. Schenker<sup>c</sup>,  
 D. Sinclair<sup>f</sup>, K. Skarpaas<sup>g</sup>, G. Smirnov<sup>e</sup>, V. Stekhanov<sup>e</sup>,  
 V. Strickland<sup>f</sup>, C. Virtue<sup>i</sup>, K. Wamba<sup>g</sup>, J. Wodin<sup>d,4</sup>

<sup>a</sup>*Department of Physics and Astronomy, University of Alabama, Tuscaloosa AL, USA*

<sup>b</sup>*Institute for National Measurements Standards, National Research Council Canada, Ottawa ON, Canada*

<sup>c</sup>*Institut de Physique, Université de Neuchâtel, Neuchâtel, Switzerland*

<sup>d</sup>*Physics Department, Stanford University, Stanford CA, USA*

<sup>e</sup>*ITEP, Moscow, Russia*

<sup>f</sup>*Physics Department, Carleton University, Ottawa ON, Canada*

<sup>g</sup>*Stanford Linear Accelerator Center, Menlo Park CA, USA*

<sup>h</sup>*Physics Department, Colorado State University, Fort Collins CO, USA*

<sup>i</sup>*Department of Physics, Laurentian University, Sudbury ON, Canada*

<sup>j</sup>*Department of Physics, University of Maryland, College Park MD, USA*

<sup>k</sup>*Physics Department, University of California, Irvine CA, USA*

---

## Abstract

The Enriched Xenon Observatory (EXO) will search for double beta decays of  $^{136}\text{Xe}$ . We report the results of a systematic study of trace concentrations of radioactive impurities in a wide range of raw materials and finished parts considered for use in the construction of EXO-200, the first stage of the EXO experimental program. Analysis techniques employed, and described here, include direct gamma counting, alpha counting, neutron activation analysis, and high-sensitivity mass spectrometry.

*Key words:* radiopurity, trace analysis, neutron activation analysis, mass spectrometry, mass spectroscopy, germanium counting, alpha counting, low background, double beta decay, EXO, EXO-200

*PACS:* 82.80.Jp, 14.60.Pq, 23.40.-s, 23.40.Bw

---

## 1 Introduction

This work was motivated by the Enriched Xenon Observatory (EXO), a multi-stage experimental research program with the purpose of detecting rare double beta decays in  $^{136}\text{Xe}$  [1]. With EXO-200, the first stage of the project, we will search for these decays in an underground cryogenic time-projection chamber (TPC) filled with approximately 200 kg of liquid xenon enriched to 80% in  $^{136}\text{Xe}$ . The EXO-200 detector is shown in Fig. 1 and described in more detail in Ref. [2]. To reach the desired half-life sensitivity of about  $6 \times 10^{25}$  yr for the 0-neutrino decay mode, the background rate of candidate events (single-site events within  $2\text{-}\sigma$  of the Q value of 2458 keV [3]) cannot exceed about 20 events per year. The background rate for the 2-neutrino decay mode should not exceed about 30 000 events per year between a threshold of approximately 400 keV and the Q value. Similarly strict background requirements are common to other double beta decay and rare-event detectors. To achieve very low background rates, all materials present in the detector, and even some external materials that are in the path of the xenon circulation or the cryogenic fluid handling, must be selected to have very low intrinsic concentrations of radioactive impurities, especially the naturally occurring elements K, Th, and U. We performed an extensive campaign of radiopurity measurements to search for and certify a library of suitable materials for every component of the EXO-200 detector. Special attention was given to materials considered for massive parts of the detector and for materials near the active volume or in contact with the xenon.

---

<sup>1</sup> Now at Center for Ion Beam Physics, Swiss Universities for Applied Physics, La Chaux-de-Fonds, Switzerland

<sup>2</sup> Now at IPHC, Université Louis Pasteur, CNRS/IN2P3, Strasbourg, France

<sup>3</sup> Now at Columbia University, New York NY, USA

<sup>4</sup> Now at Stanford Linear Accelerator Center, Menlo Park CA, USA

Our techniques for measuring intrinsic purities include mass spectrometry (MS), neutron activation analysis (NAA), and direct gamma counting. In addition, alpha counting was used to determine  $^{210}\text{Pb}$  concentrations in lead. Measurement techniques used for specific samples were selected based on a number of factors and constraints. Both NAA and MS can be used with small sample masses, on the order of a gram. In comparison to NAA, mass spectrometry is less expensive and faster. Glow-discharge mass-spectrometry (GD-MS) gives results for many elements simultaneously but has relatively poor sensitivities and can only be used with conductive or semi-conductive solids. In contrast, inductively-coupled plasma mass spectrometry (ICP-MS) can have much higher sensitivities, but the difference is large only if preconcentration procedures are used. Only materials which are chemically compatible with these procedures are candidates for ICP-MS. For our U and Th ICP-MS analyses, this implies that samples must be soluble in  $\text{HNO}_3$  or possibly in some other acids. NAA can be performed on small samples of many types of materials and can, in some cases, produce the best sensitivities of all known techniques, but the process is relatively costly and slow. Depending on the composition of the material, activation signals from the primary constituents or from uninteresting trace contaminants can interfere with the signals of interest, often resulting in higher than ideal or even useless sensitivity levels. Finally, direct gamma counting can be used to simultaneously measure levels of K, Th, and U (as well other radioactive isotopes) in virtually any material, but requires large sample masses and long measurement times.

MS and NAA assay directly the  $^{232}\text{Th}$  and  $^{238}\text{U}$  concentrations. However, these isotopes decay initially through low-energy decays below the EXO-200 threshold and through alpha emissions which, as well as having very short ranges, can be rejected by comparison of ionization and scintillation signals. It is subsequent decays of particular daughter isotopes which produce high energy gamma emissions that can penetrate into the detector's interior and contribute to the EXO-200 backgrounds. If all isotopes in a decay chain remain within the same volume, then secular equilibrium is achieved. The activity, and thus concentration, of any isotope can then be inferred from a measurement of the activity or concentration of any other isotope within the same decay chain. However, chemical processes or outgassing can remove radioactive daughter isotopes from materials, thus breaking secular equilibrium. Gamma counting has the advantage that it measures the gamma intensities of the decay products relevant to the EXO-200 backgrounds. For consistency though, data from all techniques used are reported here as total concentrations of the element corresponding to the progenitor isotope. Gamma counting results have thus been converted assuming secular equilibrium in the decay chain. For each of K, Th, and U, natural terrestrial abundance ratios were used to convert from isotopic to total elemental abundances.

Differences in the measurement techniques were weighed against our resources

and our requirements for each material. Results are listed in Tables 2 and 3. The tables also include some data (clearly identified) produced by commercial laboratories using similar techniques.

The liquid-xenon TPC of the EXO-200 detector is contained in a thin-walled copper pressure vessel. However, in various phases of the design, we have considered other materials for construction of the vessel. These included quartz, high-purity copper, fluoropolymers, and other plastics. Using NAA, described in Section 5, we found some fluoropolymers, (especially DuPont Teflon TE-6472) in their raw forms, to be among the cleanest solids that we are aware of, both from a radio-purity perspective and also from a general chemical-purity perspective. After careful review and oversight of the sintering process, we also found that finished parts could be produced cleanly. Table 3 entries 41–56 list results for various fluoropolymers in raw form as well as finished products, in some cases both before and after reviewing the sintering process. Detailed descriptions of functional studies of fluoropolymer test vessels are described in Ref. [2].

The TPC contains wire grids for charge collection, and avalanche photo diodes (APDs) for detection of scintillation light. Copper-clad flexible circuits, used in the manufacturing of various signal cables, were analyzed in two steps. First the copper was dissolved in  $\text{HNO}_3$  and measured using ICP-MS. The remaining polyimide substrate was then measured using NAA. Germanium counting was also used to analyze whole, unaltered samples of these circuits. Commercial photo-etching processes were investigated for production of the grid wires and APD contacts. Again, by careful oversight, including testing and selection of chemicals (see Table 3 entries 90–96) used in the etching process, we were able to improve the cleanliness of the products. Materials used in the construction of the APDs, including the silicon substrate and the evaporated metal coatings, were individually studied to improve on the cleanliness of the product. Results for APDs produced by Advanced Photonix Inc. (API), using their default material suppliers, are shown in Table 3 entries 131–134. Entries 121–123 show results for aluminum used in the APDs (used in both the Au contacted and Al contacted APDs) and supplied by API’s default supplier. Entries 115–120 list measurement results for aluminum replacement candidates procured by EXO.

The EXO-200 TPC is surrounded by a cryogenic heat transfer fluid (HTF) which serves as a thermal bath and also as a hermetic clean radiation shield. The HTF is contained and cooled in a large copper cryostat surrounded by lead shielding and placed underground in the Waste Isolation Pilot Plant (WIPP) near Carlsbad, NM. Because of the large mass of the HTF (approximately 4.2 tonnes), we made extra efforts to select and certify candidate materials for this use. Measurements of the final candidate material, 3M HFE-7000, are described in more detail in Section 6. Finally the copper cryostat contain-

ing the HTF is surrounded by a thick layer of lead shielding. Measurement and selection of lead at every stage of the production process is described in Section 7.

Many other raw materials and parts were studied including vacuum grease, paint, nuts, bolts, and o-rings. All measurements were selected and prioritized as needed for the specific construction and scheduling needs of EXO. In some cases, materials with unknown origins were tested for use in EXO-200. We report these results here because they give useful impressions of the general trends and achievable purity levels in various types of materials.

## 2 Handling and Surface Cleanliness

Surface cleanliness of all samples is a concern for all analysis methods used. Although we normalize most results to the sample masses, assuming that the concentrations are intrinsic to and homogenous throughout the materials, it is clear that positive readings can also come from surface contaminants.

For measurements of raw materials, extensive surface cleaning was performed and samples were handled in cleanroom environments. Typical cleaning procedures included extended soaking in solvents with sonic agitation, as well as extended soaking in 0.1 to 3 M (or higher for NAA preparation of some materials) nitric acid solutions with certified purity levels. Within a few variations, depending on the material properties, cleaning procedures were followed consistently to assure reproducibility. The effectiveness of the cleaning procedures is demonstrated by the stringent contamination limits set by the most sensitive measurements of the cleanest materials.

When analyzing finished parts (nuts, bolts, o-rings, etc.), care was taken to match the cleaning procedures of the analysis techniques to those that were or will be used for the actual installed parts. In most cases these procedures were similar to those used for analysis of raw materials. In some cases however, due to time, volume, or integrity constraints, it was not possible to perform the full cleaning procedure. Especially for non-critical parts with relatively high tolerable activities, if the parts could be well certified using less stringent cleaning procedures, then some burden or concern could be removed from the construction process.

Specifically, most EXO-200 finished parts were surface cleaned using the following treatment with high purity solvents targeting organic, metallic, and ionic surface impurities:

- (1) Acetone rinse followed by ethanol (or methanol) rinse to remove any

Sample	Th [pg/cm <sup>2</sup> ]	U [pg/cm <sup>2</sup> ]
Xenon piping, burst disk, after cleaning <sup>a</sup> .	5.8 ± 0.2	1.2 ± 0.1
Bottom inner surface of outer cryostat, before cleaning <sup>a</sup> .	380 ± 5	140 ± 3
Top inner surface of outer cryostat, before cleaning <sup>b</sup> .	2.6 ± 0.2	0.46 ± 0.04
Top outer surface of outer cryostat, after cleaning <sup>b</sup> .	0.60 ± 0.09	0.21 ± 0.05
Jehier super insulation from top of cryostat, after alcohol rinse <sup>b</sup> .	5.9 ± 0.2	1.6 ± 0.1
Wessington Cryogenics HFE storage dewar, manufacturer cleaning with wipes soaks and pressure washing <sup>a</sup> .	215 ± 12	43 ± 6

Table 1

Th and U surface contamination as determined by wipe testing. Blanks have been subtracted.

<sup>a</sup> The filter was wetted with ethanol before wiping.

<sup>b</sup> The filter was wetted with 0.1 M HNO<sub>3</sub> before wiping.

grease left over from machining or touching. Small parts underwent ultrasonic cleaning for about 15 minutes while immersed in each solvent, often followed each time by a rinse in the same solvent.

- (2) 0.1 to 1 M HNO<sub>3</sub> rinse to dissolve metallic contamination. For metallic parts light etching results in removal of the surface. Small parts were fully immersed in acid.
- (3) Deionized water rinse following the etch. Small parts were dried in a vacuum oven; large parts were left to dry in a cleanroom.

For thin photo-etched phosphor-bronze TPC parts, we found high levels of U which appeared to be surface contamination resulting from the commercial etching procedure. We were able to reduce the U levels by requesting the use of fresh chemicals in the etching process (compare entries 93 and 94 of Table 3) in combination with use of an expanded cleaning procedure which we developed to maximize cleaning effectiveness while minimizing loss of material. These parts were first rinsed in methanol followed by deionized water and then rinsed three times in 3 M HNO<sub>3</sub> for 10 minutes, followed each time by a further rinse in deionized water. This procedure was used to obtain the result in Table 3 entry 89; a 15% loss of sample mass was observed.

After surface cleaning, parts were double bagged (when practical according to size) and were only touched with disposable powder free gloves to prevent re-contamination.

Surface cleanliness of large parts was directly verified by means of wipe testing with Whatman 42 paper filters. The Th and U content of the filters was determined, after ashing, by means of ICP-MS. To reduce the blank concentrations, the filters were soaked for 24 h in 1 M HNO<sub>3</sub> followed by thorough

rinsing with deionized water and drying. Analysis of blank filters yielded Th and U masses of  $0.27 \pm 0.06$  and  $3.0 \pm 0.6$  ng per filter respectively before acid cleaning and yielded  $0.31 \pm 0.02$  and  $0.15 \pm 0.03$  ng after acid cleaning. To facilitate transfer of surface activity onto the filter paper, the surface to be tested was wetted with either alcohol or 0.1 M nitric acid. The fluid was spread over some surface area and then absorbed with the filter paper. Blank filters were always analyzed to control the filter paper background.

After drying, the filter paper samples were accurately weighed, transferred into porcelain crucibles, and placed in a muffle furnace at  $200^{\circ}$  C for 20 minutes. The temperature of the furnace was then gradually raised at a rate of approximately  $10^{\circ}$  C/min with pauses for 30 minutes at  $300^{\circ}$  C and  $400^{\circ}$  C and finally raising the temperature to  $500^{\circ}$  C where it was maintained for about one hour. The crucibles were then removed from the furnace and allowed to cool down. After the samples were cooled, 10 ml of 3 M nitric acid was added to each crucible, evaporated to near dryness on a hotplate, and reconstituted to 10 ml with 0.5% nitric acid. The Th and U content of the filters was determined by means of ICP-MS. Recovery tests were performed where the filter papers were spiked with known concentrations of the analytes. Complete recovery ( $> 94\%$ ) was obtained.

Table 1 summarizes the results for various wipe tests performed on EXO-200 samples.

### 3 Mass Spectrometry

Inductively-coupled plasma mass spectrometry offers sub pg/ml detection limits for U and Th with minimal analysis time. However, one of the main limitations of this technique is the need for sample preparation prior to analysis, as higher levels of matrix components can give rise to deposition of matrix constituents on the sampler and skimmer cones of the spectrometer. Thus, a dissolved sample may need to be diluted in order to lower its total dissolved solids content to  $< 1\%$ , clearly degrading achievable detection limits. One way of overcoming this drawback is to undertake prior separation of the analytes from the matrix. Several methods have been used for this purpose including coprecipitation [5,6,7], liquid-liquid extraction [8,9,10], distillation [11], and ion-exchange [12,13] which was used in this work (see Sec. 3.1). These techniques often require longer analysis times and give rise to additional analytical problems, including contamination during sample pretreatment and increased blank levels, which must be carefully controlled.

Direct analysis of solid samples can be advantageously performed, without chemical sample preparation, by glow-discharge mass spectrometry (GD-MS)

[14,15] wherein the sample functions as the cathode of the discharge, making this approach particularly suitable for the analysis of high-purity metals.

### 3.1 ICP-MS

An ELAN DRC II (dynamic reaction cell) ICP-MS (Perkin-Elmer Sciex) equipped with a cyclonic glass spray chamber and a pneumatic nebulizer (Meinhard) was used for the determination of U and Th with sensitivities as low as  $10^{-12}$  g/g. The ICP-MS operating parameters were selected to maximize sensitivity for U and Th. Samples were acid digested and then the analytes separated using a chromatography resin (UTEVA from Eichron). The U fraction was eluted from the resin with 15 ml of 0.02 M HCl, and the Th fraction was subsequently eluted with 30 ml of 0.5 M oxalic acid. Both fractions were evaporated to near dryness; the thorium fraction was decomposed with 24 ml of a mixture of concentrated HNO<sub>3</sub>/30% and H<sub>2</sub>O<sub>2</sub> (1:1). Both fractions were reconstituted to 2 ml with 0.5% nitric acid. U and Th were measured at masses 238 and 232 respectively. The procedure is described in more detail in Ref. [16].

For the determination of K concentrations at levels below  $10^{-6}$  g/g, samples were acid digested, diluted 100-fold and subsequently analyzed by DRC-ICP-MS using an ultrasonic nebulizer as a sample introduction system. <sup>39</sup>K suffers from interferences from <sup>38</sup>Ar <sup>1</sup>H<sup>+</sup> and <sup>40</sup>Ar. These interferences were overcome with the use of chemical resolution, a process used to selectively remove interfering polyatomic or isobaric species from the ICP-MS ion beam using controlled ion-molecule chemistry. Ammonia (at 0.5 ml/min flow rate) was used as a reaction gas as it reacts with the Ar-based interferences to form new species that do not interfere with <sup>39</sup>K. Samples were introduced to the ICP-MS with an ultrasonic nebulizer in order to further decrease the hydride formation and consequently the interference to <sup>39</sup>K. The samples were nebulized by a piezoelectric crystal transducer. The nebulized aerosol was passed through a heated chamber and condenser where the solvent vapor was removed.

Uncertainties in the ICP-MS results were dominated by variability in the subtracted backgrounds, as observed by analysis of clean digestion acids, and to a lesser extent by scaling errors due to calibration uncertainties. All known uncertainties are included in the tabulated results.

### 3.2 GD-MS

A VG 9000 glow discharge mass spectrometer (Thermo Electron Corp., UK) was used for direct analysis of solid samples (conducting and semiconducting



solids). The instrument is capable of detecting impurities directly in the solid from the percent level down to below  $10^{-9}$  g/g in a single run, allowing for a rapid turn around of submitted samples. It relies on a DC glow discharge ion source coupled to a high resolution magnetic sector analyzer in reverse Nier Johnson geometry with electron multiplier detection at nominal resolution  $R = 3000$ , where  $R \equiv m/\delta m$ , and  $\delta m$  is the resolvable mass difference at an ion mass of  $m$ . Atoms were sputtered in a low-pressure DC argon discharge, subsequently ionized in this plasma, and extracted into the mass spectrometer for separation and detection. Test portions of the samples were prepared by cutting pins of approximately  $2.5 \times 2.5 \times 20$  mm and subjecting them to a careful surface leach in dilute ultrapure nitric acid. Following a rinse with ultrapure water, the samples were permitted to air dry in a laminar-flow class-100 clean-bench, where they were subsequently mounted into the DC ion source. Once under vacuum, and then Ar purged, the glow discharge was ignited. Any surface contamination on the test samples was removed by a 30 minute pre-burn in the plasma before data acquisition was initiated. Typically 300 mass spectral scans were acquired, each having a 50 ms dwell or integration time. The GD-MS instrument was calibrated with the use of a variety of reference materials used to establish relative sensitivity factors to provide semiquantitative analysis, results of which are deemed to be (conservatively) within a factor of 2 of the real value of the concentration of the analyte. GD-MS is free from the matrix dependence response plaguing most other elemental analysis techniques, minimizing the need for matrix matched standards.

## 4 Gamma Counting

For EXO, gamma counting was used primarily for small non-critical components, such as screws, washers, etc., which contribute little to the EXO-200 detector mass. This technique was also used for cross checking other measurements of bulk materials, in particular measurements of the copper for the TPC vessel and cryostat, and of the shielding lead.

A few non-critical materials were counted in above ground detectors but most were counted underground in the Vue-des-Alpes underground laboratory. The overburden is 230 m of rock (600 m.w.e.), so that the nucleonic component of the cosmic rays is completely eliminated. The muon flux is attenuated by a factor of 1000. The detector itself is a p-type coaxial germanium detector with a useful volume of 400 ml. The geometry is indicated in Figure 2. The germanium crystal is housed in a cryostat made from highly purified Pechiney aluminum. All materials entering in the construction of the detector were themselves selected for low activity. The energy resolution is 2.2 keV at 2 MeV. The detector is protected against local activities by a shielding composed of 15 cm of OFHC copper and 20 cm of lead. The shielding is contained in an

air-tight aluminum box which is slightly overpressurized with boil-off nitrogen from the detector's liquid-nitrogen dewar, thus preventing radioactive radon gas from entering the detector volume. As shown in Fig. 2, a small volume is free around the sensitive part of the detector in order to position samples to have the best possible solid angle. Small samples were placed on top of the cryostat whereas larger ones were arranged on top and around the cylindrical part of the cryostat. This arrangement has the extra advantage that it reduces self absorption of gammas in the sample.

Prior to insertion, samples were ultrasonically cleaned in an alcohol bath. Data taking was started one day after closing the shielding to ensure that all radon gas was flushed out. Normally data were accumulated for a period of one week for each sample. Detector backgrounds limit the effectiveness of longer accumulation times. In critical cases, (measurements of lead and copper) data were accumulated for periods as long as a month. The contribution of a sample is obtained by subtracting the background spectrum taken without any sample (Figure 3). The background was measured at regular intervals although it was found to be very stable.

For each sample, the geometry was entered in a simplified way into a GEANT3 based Monte Carlo simulation which contained also the detector configuration. The acceptance as a function of energy of the full energy gamma peaks was computed and used to translate the observed intensity of a transition, or the upper limit on it, into a specific activity. The computed acceptance was cross checked by exposing the detector to calibrated gamma sources. The sensitivity depends on the sample mass and configuration, which affect the solid angle and the self absorption. For transitions with several gamma emissions contributing in parallel, or by cascade, the peak intensities were combined. The best sensitivity was achieved with copper samples with masses of several kilograms (see Table 3 entry 2). The quoted errors include statistical uncertainties as well a systematic error, dominated by the acceptance, which is estimated to be of order 10 %.

## 5 Neutron Activation Analysis

We have used the MIT Reactor (MITR) Lab to neutron activate many material samples. After activation and shipping, gamma emissions from the unstable activation products were observed at an EXO lab using the same germanium detector as that used for the above ground direct gamma counting mentioned in Sec 4. By observing gamma energies, intensities, and decay half-lives it is possible to identify and measure the activities of many of the neutron activation products. In practice, good spectral analysis in the presence of a multitude of gamma lines is not trivial and can have a significant impact on sensitivity

and accuracy.

In order to maximize use of data (and thus sensitivity), as well as to simplify the analysis, a spectral fit was constructed using the most global set of experimental parameters as was practical. Multiple energy regions of interest were defined, each having three background parameters. Two parameters for a linear energy-calibration and two global energy-dependent peak-width parameters were used in the fit as well as one activity parameter for each isotope. Care was taken to convert energy regions of interest to channel regions in a way which would not change the data set while minimizing the fit, which included the calibration parameters. Peaks were defined with fixed energies, and each rate was associated with an isotopic activity via the product of the branching ratios and the detector efficiency at the relevant energy. By parameterizing activities instead of peak areas, all peaks associated with a single isotope could be used to simultaneously constrain an activity. The inclusion of strong, known peaks in the fits resulted in automatic energy and resolution calibration. Interleaved calibration data could also be used to introduce constraint terms for particularly in-active samples after long delay times. By allowing the energy calibration to float in a constrained manner while keeping peak energies fixed, subtleties of explicitly constraining peak centroids were avoided, and strong correlations in peak-position uncertainties were retained. The fit procedure was automated to produce results for data files taken in temporal sequence. This produced time-dependent decay curves for each activity which could be fit to determine initial activities and half lives. A calibration gamma spectrum taken from the interactive software interface is shown in Fig. 4. The time series of different activities shown in Fig. 5 were found by combining the data from this and other spectra collected in sequence.

Elemental concentrations were inferred using tabulated neutron capture cross sections folded with a standard reactor neutron spectrum. We assume that the relative isotopic abundances within the samples are given by the natural terrestrial abundance ratios. The reactor neutron flux was periodically calibrated by activating samples of NIST coal fly-ash Standard Reference Material 1633b, which has certified known concentrations of several NAA-detectable elements including K, Th, and U. Repeated calibrations showed a linear correlation between reactor power and thermal neutron flux. For activation runs without a fly-ash calibration sample, this correlation was used together with the stated reactor power at the time of activation. The fractional flux of epi-thermal neutrons was found to have only little dependence on the reactor power. Due to the large resonance integral in the neutron capture cross section of  $^{238}\text{U}$ , this nuclide is quite sensitive to this detail. Results listed in Table 3 include a statistical uncertainty and a systematic uncertainty, which in most cases is dominated by a 10% error associated with flux variations and with solid angle variations during germanium counting.

After demonstrating good reproducibility over the course of several years, calibrations were recently performed only about once per year. However, the latest calibration, performed in September of 2006 showed that the ratio of total flux to epi-thermal flux was about a factor of 3 lower than found in the previous calibration, performed in March of 2005. Data taken in the interval between these two calibrations are thus subject to significantly higher systematic uncertainties. The affected measurements are indicated in Table 3. The quoted results use the original 2005 calibration and do not include this added flux uncertainty. Using the 2006 calibration, results are found to be higher by factors of approximately 1.1, 1.3, and 2.2 for K, Th and, U respectively.

NAA results using the same facility and essentially the same techniques have been reported in the past [17] in more detail. In Ref. [17], NAA measurement limits on the order of  $10^{-14}$  g/g to  $10^{-15}$  g/g of Th and U were achieved for KamLAND liquid scintillator, demonstrating the potential power of the technique. However, achieving these sensitivities required a specialized measurement campaign customized to the material of interest. Specifically the preconcentration and chemical separation techniques used in Ref. [17] were not employed, with one exception described below, for measurements in the present work. When surveying a large number of samples, such specialized techniques are not practical. Many systematic details of the technique including sample mass, containment vessel choice, and irradiation time, were varied to account for properties of individual materials and our specific analysis needs and goals.

## 6 Heat Transfer Fluid

3M Novec HFE-7000, 1-methoxyheptafluoropropane, serves as a heat transfer fluid and as passive shielding in EXO-200. Because of its large mass and close proximity to the active detector volume, the allowable tolerances for U and Th contamination in this material are particularly stringent. An extended effort was made to improve analysis sensitivities for this material. Initially a standard neutron activation analysis was performed producing limits for K, Th, and U concentrations which were among the lowest of any of the materials measured (see Table 3 entries 135–138). We also found that HFE-7000 has very low levels of other foreign elements, making it one of the most pure materials that we have studied.

In order to make further improvements we preconcentrated the HFE-7000 by evaporation, reducing its mass by a factor of 1000. We attempted to quantify the Th and U retention of the evaporation process by mixing organo-metallic standards [17] with the HFE-7000. These studies were unsuccessful, but indicated a very low solubility of actinides in HFE-7000. For indirect verification

of metal retention,  $^{220}\text{Rn}$  gas was bubbled through an HFE-7000 mixture. This loaded the HFE-7000 with  $^{212}\text{Pb}$  which was detectable in a gamma detector before and after evaporation. The concentrate was transferred from the evaporation vessels to a separate test tube and further evaporated to produce a dry residue. Approximately 20% of the  $^{212}\text{Pb}$  was retained in the concentrate residue. With large systematic uncertainties, the amount of  $^{212}\text{Pb}$  on the surfaces of the evaporation vessels was found to be consistent with the remaining 80% of  $^{212}\text{Pb}$  initially introduced. With the assumption that this 20% evaporation retention also applies for Th and U, we derived strict limits for their concentrations in HFE-7000 as shown in Table 3 entry 139.

## 7 Shielding Lead

To find a suitable shielding lead we needed to select, as usual, for low concentrations of K, Th, and U, but also for low levels of  $^{210}\text{Pb}$ .  $^{210}\text{Pb}$  and its shorter lived decay product  $^{210}\text{Po}$  are primarily beta and alpha emitters respectively. However, because of their potentially high activities, long ranged Bremsstrahlung radiation as well as a very weak gamma line at 803 keV can potentially penetrate shielding at rates high enough to impact EXO-200 backgrounds in the energy range of the  $^{136}\text{Xe}$  two-neutrino decay mode.

To address this additional concern we used a 1700  $\text{mm}^2$  ion-implanted silicon detector to observe the 5304 keV alpha particles from the decay of  $^{210}\text{Po}$  (the decay product of  $^{210}\text{Pb}$ ) in several different supplies of lead. The detector efficiency was calibrated with Doe Run lead batches previously analyzed by Physikalisch-Technische Bundesanstalt (PTB) in Germany. Background measurements were taken by replacing the lead samples with a silicon wafer.

The EXO-200 shielding lead was selected, acquired, smelted, cleaned, and machined at JL Goslar in Germany. Many batches of Doe Run lead were smelted together into three homogenized batches. We analyzed the  $^{210}\text{Po}$  activities of samples from all candidate batches (about 20) of Doe Run lead purchased and from samples of all three homogenized batches. We found that the  $^{210}\text{Po}$  activities of most candidate batches varied only within the roughly 20% measurement uncertainty. A few batches varied by as much as 50%, and ultimately 3 batches were thus rejected before homogenization. In table 2 we report the analysis results of levels of  $^{210}\text{Pb}$  in the EXO-200 lead as well as other lead varieties studied. Alpha spectra from lead samples are shown in Figure 6 along with a background spectrum.

All candidate Doe Run batches and all homogenized batches were tested for K, Th, and U levels using GD-MS analysis. Selected batches, including all of

<b>Lead Source</b>	<b>Activity [<i>Bq/kg</i>]</b>
JL Goslar, Doe Run, EXO smelting lot 3-708.	20±5
JL Goslar, Doe Run, EXO smelting lot 3-707.	17±5
JL Goslar, Doe Run, EXO smelting lot 3-706.	17±4
JL Goslar, un-smelted Doe Run lot 9273.	25±4
Tako Esco Ltd.	165±33
JL Goslar, Boliden.	18±3
Plombum, VG1.	5.9±0.9
Plombum lead from Integrated Ocean Drilling Program	5.4±1.3
JSC Industrial Corporation, lead quality C1.	1265±183

Table 2  
 $^{210}\text{Po}$  (from  $^{210}\text{Pb}$  decay) activities in various lead sources as measured by alpha counting.

the homogenized batches, were further tested using ICP-MS, which provided higher sensitivity to the uranium and thorium content. All three homogenized batches were found to have levels of K less than  $7 \cdot 10^{-9}$  g/g and both Th and U levels below  $< 1 \cdot 10^{-12}$  g/g. However, a few of the original candidate Doe Run batches did show levels higher than these limits. Some of these were rejected for use in forming the EXO lead.

## 8 Summary

Previous attempts to reduce intrinsic radioactive backgrounds in detector systems have generally focused on studies of a few common primary construction materials such as copper and lead. In order to facilitate development of complex low-background detector systems, clean materials must be available for producing a wide variety of parts. We have performed a systematic study of trace radioactive impurities in a large variety of parts and materials, focusing on those required to construct the EXO-200 cryogenic TPC detector system (See Table 3). As well as finding suitable raw materials and commercially available parts, we have also shown quantitatively that efforts to improve cleanliness of the production and handling of parts can result in measurable improvements in radiopurity. We hope that these studies will help to facilitate the advancement and development of the next generation of low-background counting facilities, both by helping to reduce background levels below what has previously been achieved, and by allowing the construction of more complex purpose-built detection systems.

## Acknowledgements

We thank Dirk Arnold at PTB for contributed data, Kenji Kingsford at Saint Gobain for extensive help with Teflon selection and finishing, as well as Niel Washburn, Richard Van Ryper, and Sharon Libert at DuPont for consultations and generous materials donations. We thank Edward Lau, Susan Tucker and Judith Maro at MITR as well as David Woisard, APT, API, and Vaga Industries for their accommodating cooperation. This work was supported in part by the US Department of Energy under contract number DE-FG02-01ER4166.

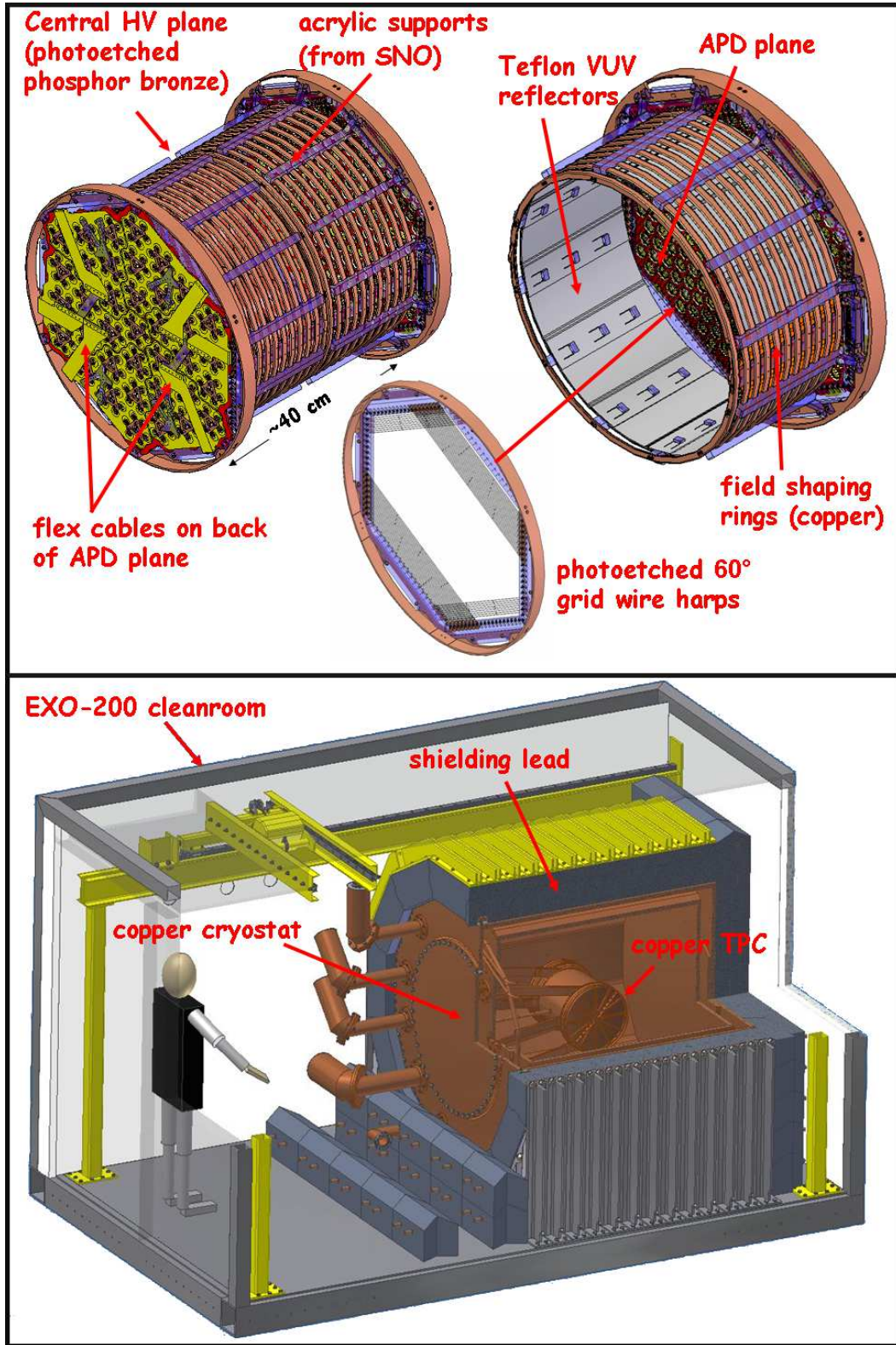


Fig. 1. Top panel: The EXO-200 TPC with major internal parts shown. Bottom panel: Cut-away view of the TPC housed in the shielded cryostat. The cleanroom is underground in the Waste Isolation Pilot Plant (WIPP) near Carlsbad, NM. with an overburden of  $1585^{+11}_{-6}$  m.w.e. [4].



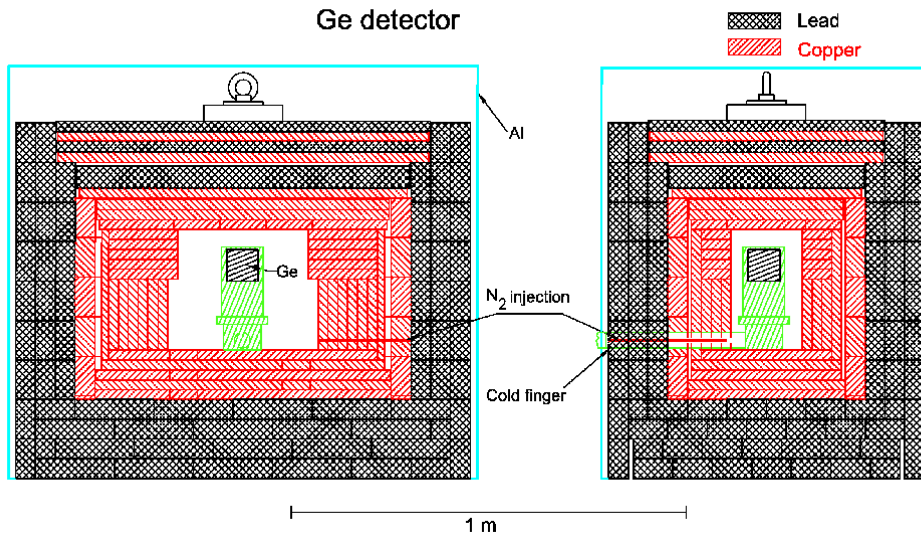


Fig. 2. The germanium detector in its copper and lead shielding. The aluminum radon containment box is also shown.

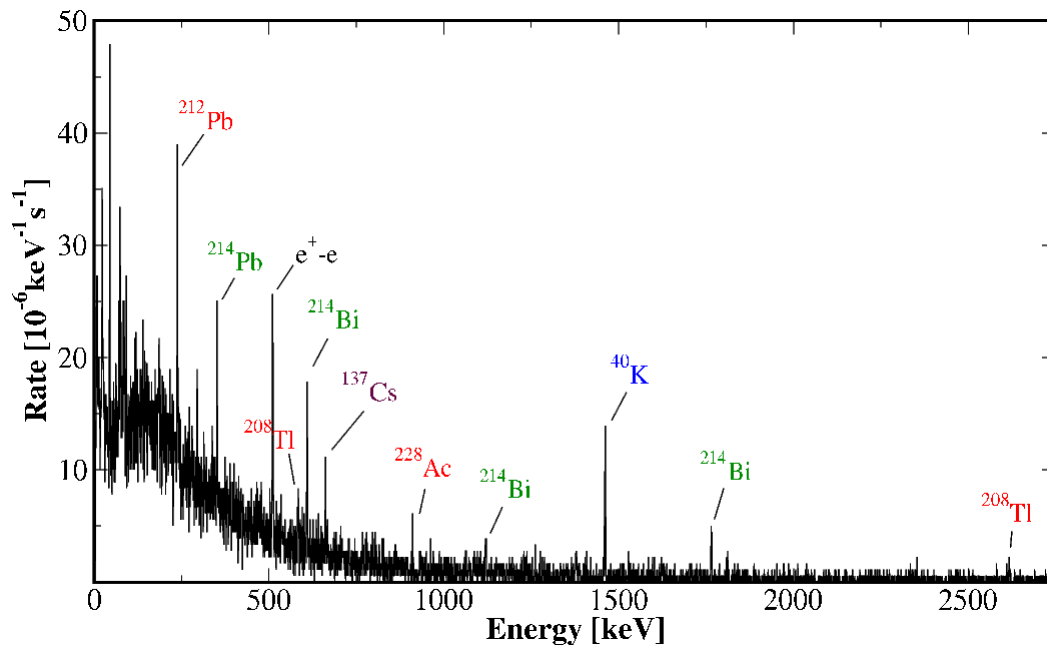


Fig. 3. Underground germanium background spectrum, measured with no sample for 672 h. Gamma lines from natural activities, namely the  $^{232}\text{Th}$  ( $^{208}\text{Tl}$ ,  $^{228}\text{Ac}$ ,  $^{212}\text{Pb}$ ) and  $^{238}\text{U}$  ( $^{214}\text{Bi}$ ,  $^{214}\text{Pb}$ ) chains,  $^{40}\text{K}$ , as well as the  $^{137}\text{Cs}$  line from an artificial activity, are indicated.

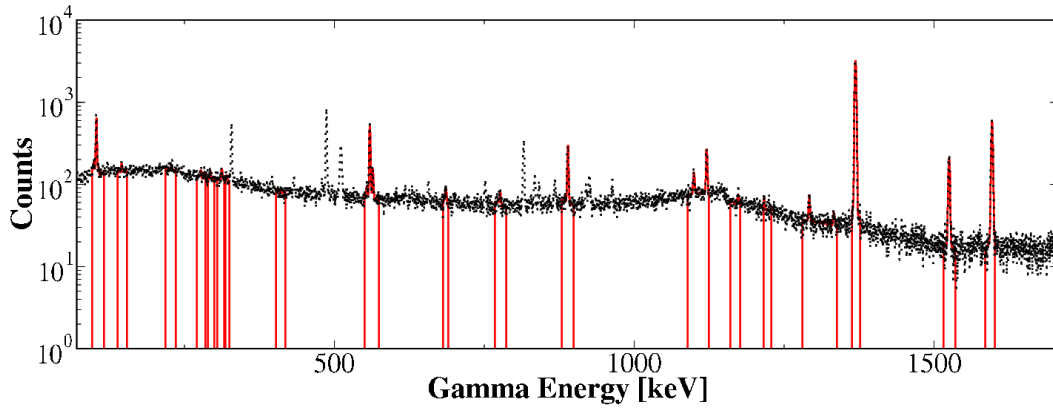


Fig. 4. Partial neutron-activated fly-ash gamma spectrum (dotted line) with global fit (solid line). The parameterization for this fit described backgrounds for 23 regions of interest and 62 peaks with rates linked to 31 activity parameters.

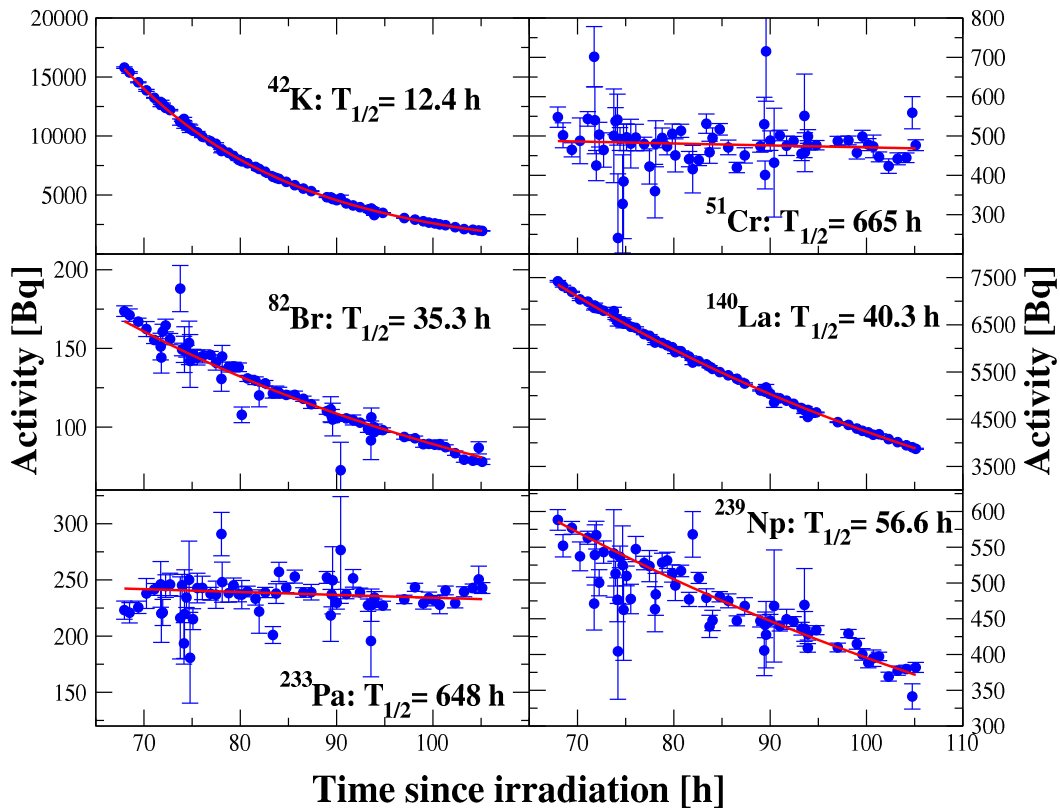


Fig. 5. Time development of activities in a neutron-activated fly-ash calibration sample as determined from a sequence of spectral fits (See Figure 4). The points are the data; the curves are fit to exponential decays with the half-lives fixed to the values shown.

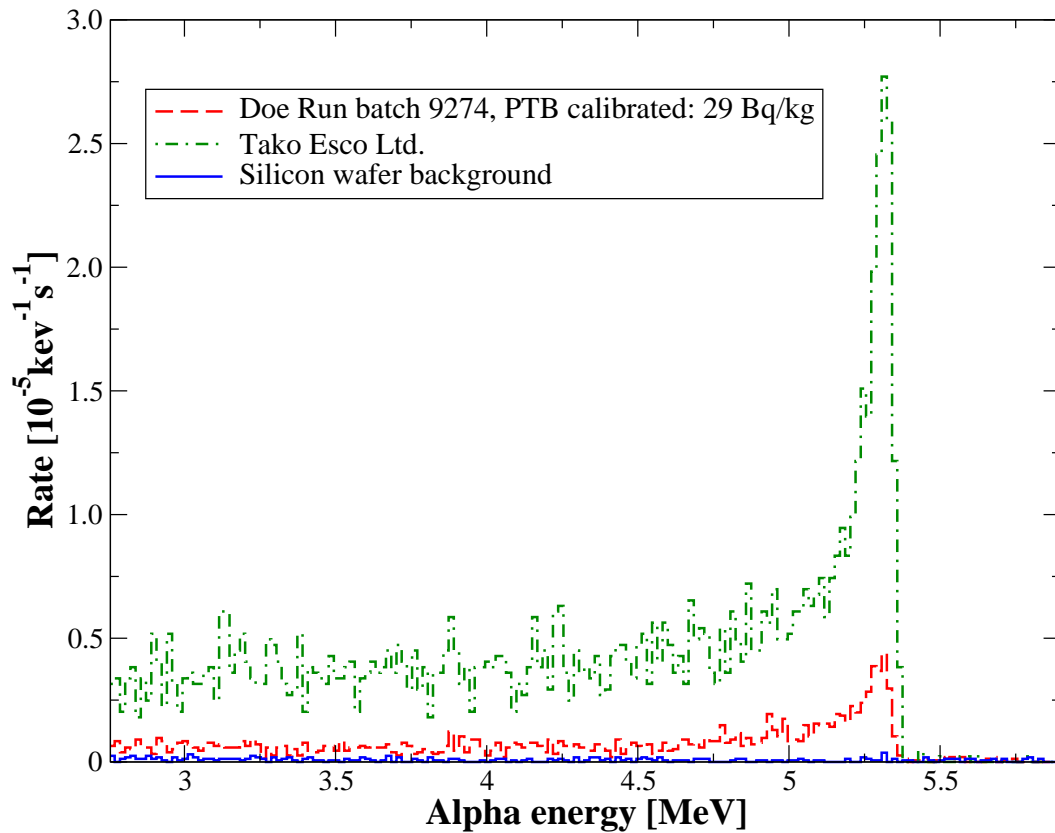


Fig. 6. Spectra from alpha counter including Doe Run batch 9274, which was a calibration batch measured by PTB ( $28.9 \pm 2.9$  Bq/kg), as well the spectrum from lead supplied by Tako Esco Ltd., and a background spectrum. The spectra are binned in groups of ten channels.

Table 3: Measurement results for K, Th, and U concentrations in a variety of materials. Manufacturer production lot numbers or arbitrary identifiers are indicated for materials where multiple lots were studied. Uncertainties are quoted at 68% C.L. and limits are 95% C.L. Results which are less than  $3\text{-}\sigma$  above zero (not including systematic scaling uncertainties) are reported as upper limits. GD-MS measurements have a factor of two uncertainty. In the “method” column, “A.G. Ge” refers to above ground germanium counting. Measurements with methods of “Balazs Analytical Services” or “Shiva Inc.” were performed by the commercial services of the respective companies. Entries 31 and 38 list data taken from Refs. [18] and [19] respectively as indicated. Where available, germanium counting results for  $^{60}\text{Co}$  and  $^{137}\text{Cs}$  activities are given within the sample descriptions.

\* Indicated NAA results may be affected by a neutron flux calibration discrepancy described in Sec. 5. The tabulated results do not include systematic uncertainties arising from this discrepancy.

#	Material	Method	K conc. [ $10^{-9}\text{g/g}$ ]	Th conc. [ $10^{-12}\text{g/g}$ ]	U conc. [ $10^{-12}\text{g/g}$ ]
<b>Bulk Copper</b>					
1	Norddeutsche Affinerie, NOSV copper made May 2002.	Shiva Inc. GD-MS	0.4	<5	<5
2	Norddeutsche Affinerie, NOSV copper made May 2002.	Ge	<120	<35	<63
3	Norddeutsche Affinerie OFRP copper made May 2006, batch E263/2E1.	ICP-MS	<55	<2.4	<2.9
4	Norddeutsche Affinerie OFRP copper made May 2006 batch E262/3E1.	ICP-MS	<50	<2.4	<2.9
5	Rolled Norddeutsche Affinerie OFRP copper, May 2006 production. Rolled by Carl-Schreiber GmbH.	ICP-MS	-	<3.1	<3.8
6	TIG welded Norddeutsche Affinerie OFRP copper made May 2002. No cleaning after welding. Result are normalized to length of weld.	ICP-MS	-	<9.8 pg/cm	10.2±3.4pg/cm
7	Valcool VNT 700 metal working lubricant, concentrate.	A.G. Ge	38000±11000	<10000	<3700
8	Water alcohol mixture, lubricant for machining of Cu parts.	A.G. Ge	<44000	<18000	<3800
<b>Lead</b>					
9	JL Goslar cutting oil. Used for cutting 98% distilled water, 2% cutting oil. $^{60}\text{Co}$ : <1.8 mBq/kg, $^{137}\text{Cs}$ : <12 mBq/kg.	Ge	93500±1000	<790	3650±510
10	Paint for lead bricks, JL Goslar, type: Glasurit MS-Klarlack. Proportions: 2 paint, 1 hardener, 0.1 solvent.	Ge	720±170	<170	790±90
11	EXO Pb, JL Goslar smelting lot 3-706.	ICP-MS	-	<1	<1
12	EXO Pb, JL Goslar smelting lot 3-706.	GD-MS	<15	<6	<6

13	EXO Pb, JL Goslar smelting lot 3-707.	ICP-MS	-	<1	<1
14	EXO Pb, JL Goslar smelting lot 3-707.	GD-MS	<10	<5	<6
15	EXO Pb, JL Goslar smelting lot 3-708.	ICP-MS	-	<1	<1
16	EXO Pb, JL Goslar smelting lot 3-708	GD-MS	<7	<7	<8
17	JL Goslar production, Doe Run, Lot 9273.	ICP-MS	-	<3	<3
18	JL Goslar production, Doe Run, Lot 9273.	GD-MS	<5	<10	<10
19	Vulcan Lead, source Doe Run. Lot ID D9258.	GD-MS	5	<5	<5
20	Vulcan Lead, source Doe Run. Lot ID D9146.	GD-MS	5	<4	<5
21	Vulcan Lead, source Doe Run. Lot ID D9119.	GD-MS	<1	<4	<4
22	Vulcan Lead, source Doe Run. Lot ID D9086.	GD-MS	<0.5	<5	<6
23	Plombum, VG2 lead.	Shiva Inc. GD-MS	2.1	270	<100
24	Plombum, VG2 lead	ICP-MS	-	<2	<0.5
25	Plombum, VG2 lead.	GD-MS	<1	<9	<20
26	Plombum, VG2 lead.	Ge	<3.0	<11	<21
27	Plombum, VG1 lead	GD-MS	<2	<7	<10
28	Teck-Cominco low alpha lead.	GD-MS	<2	<4	<4
29	Boliden lead.	GD-MS	<4	<7	<7
30	Princess Louisa Pb (1743).	GD-MS	<0.9	<8	<10
31	Princess Louisa Pb (1743). Data from D. Arnold [18].	PTB Ge [18]	<3600	<3200	3600±740
32	JSC Industrial Corporation, lead quality C1.	Shiva Inc. GD-MS	0.52	110	<10
33	JSC Industrial Corporation, lead quality C1.	Ge	<520	790±150	8500±900
34	MUNU lead pellets. <sup>60</sup> Co: 1.4±0.3 mBq/kg.	Ge	710±120	<320	970±140
35	Cominco low alpha Pb.	NAA	-	<22	-
36	Boliden Pb.	NAA	-	<22	-

#### Plastics

37	SNO acrylic, batch 48, panel 09.	NAA*	<2.3	<14	<24
38	SNO acrylic. Data from J. Boger et al. [19]	SNO NAA [19]	-	<1.1	<1.1
39	DuPont Vespel, plaque 1.	NAA*	46±5	<21	<29
40	DuPont Vespel. plaque 2.	NAA*	209±22	<10	<19
41	Stanford stockroom virgin Teflon.	NAA	16±2	122±12	<20
42	DuPont Teflon TE-6472, raw material.	Ge	<740	<112	<200
43	DuPont Teflon TE-6472, raw material.	NAA*	1.8±0.2	<0.26	<0.78
44	APT supplied DuPont TE-6472 raw material.	NAA	2.5±0.8	<1.8	<4.4
45	Saint Gobain supplied DuPont 440-HPB PFA, raw material, lot: 0102THPP07.	NAA	<0.9	<1.9	<1.8
46	Saint Gobain supplied DuPont 440-HP PFA, raw material, lot: 0401THP053.	NAA	6.7±0.9	-	<5.9
47	Saint Gobain supplied DuPont 450-HPB PFA. Material finished using supplier's default procedures.	NAA	740±77	65±6.5	<75
48	Saint Gobain DuPont 440-HP PFA. Material finished using customized procedures.	NAA	5.3±1.0	<13.3	<3.0
49	Saint Gobain supplied Daikin Neoflon PFA AP-231SH, lot A31SR 29010 MFR 1.76, raw pellets.	NAA*	81±8	29.3±3.5	48.1±7.8
50	Saint Gobain supplied Daikin Neoflon PCTFE (Kel-F), M-400H, raw material. <sup>60</sup> Co: <0.58 mBq/kg.	Ge	<980	<570	450±100
51	Saint Gobain supplied Daikin Polyflon PTFE M-112, raw material.	NAA*	<12	<4.9	<7.0
52	Saint Gobain supplied Daikin Polyflon PTFE M-111, raw material.	NAA*	<4.9	<2.6	<7.2
53	Saint Gobain supplied 3M TFM-1700, raw material.	NAA	2220±230	-	<970
54	Saint Gobain supplied 3M TFM-1700 Teflon Material finished using supplier's default procedures.	NAA	3100±300	<5.4	<10
55	Saint Gobain supplied 3M TFM-1700. Material finished using customized procedures.	NAA	2900±300	-	<128
56	APT supplied DuPont, NXT-75 raw Teflon.	NAA	3.2±1.3	<1.6	<1.9
57	General Electric Polycarbonate 104-111N raw pellets, grade 104-111N.	NAA	107±53	<33	<105
58	Dow Corning Polycarbonate PC20010 raw pellets, grade PC20010.	NAA	18±2	<33	<6.5
59	Bayer Makrolon finished Polycarbonate plastic.	NAA	53±5	204±20	<136

60	Bayer Makrolon raw Polycarbonate pellets.	NAA	288±29	<21	<3.7
<b>Quartz</b>					
61	Corning high purity quartz.	NAA*	1.05±0.24	1.8±0.5	270±27
62	Dynasil quartz.	NAA*	1.16±0.28	-	226±22
63	Saint Gobain Spectrosil quartz.	NAA	<3	12±2	<4.6
64	Kvartzsteklo, fused silica type KY1	NAA	21±3	23±3	17±4
65	Heraeus 2 quartz.	NAA	2.0±0.5	6.7±1.2	5.5±2.2
66	Heraeus 311 quartz.	NAA	5.8±0.8	14.1±2.1	4.9±2.0
67	Heraeus Suprasil quartz.	NAA	-	59±14	21±9
<b>Adsorbends</b>					
68	Selecto 32-63 $\mu\text{m}$ Silica gel, acid washed.	A.G. Ge	<54000	63000±7600	46000±3800
69	Selecto 32-63 $\mu\text{m}$ Silica gel.	A.G. Ge	<122000	167000±96000	152000±37000
70	Selecto, Alusil 70 (alumina gel).	A.G. Ge	$(1.5\pm 0.2)\cdot 10^8$	<160000	374000±58000
71	Selecto, Alusil 40 (alumina gel) no K added.	A.G. Ge	$(5.3\pm 0.1)\cdot 10^7$	429000±78000	140000±44000
72	Cu-Mn Catalyst T-2550, Sued Chemie.	A.G. Ge	$(1.1\pm 0.1)\cdot 10^6$	146000±15500	48000±8600
73	Carbo-Act International (NL) activated charcoal.	NAA	103±11	111±18	206±22
74	Carbo-Act International (NL) activated charcoal.	A.G. Ge	<145000	<74000	<65000
75	Kansai MAXSORB activated charcoal.	NAA	496000±25000	81000±41000	-
76	Kansai MAXSORB activated charcoal.	A.G. Ge	622000±81000	205000±27000	44000±11000
<b>Phosphor-Bronze Photo-Etching</b>					
77	0.005" thick phosphor-bronze from Sequoia Metals.	ICP-MS	150±60	14±3	87±3
78	0.005" thick phosphor-bronze for TPC grid wires from E. Jordan Brooks.	ICP-MS	<80	27±2	<1
79	0.005" thick phosphor-bronze for TPC grid wires from E. Jordan Brooks. $^{60}\text{Co}$ : <0.3 mBq/kg, $^{137}\text{Cs}$ : <1.9 mBq/kg.	Ge	<460	<135	<123
80	0.01" thick phosphor-bronze for APD spiders from E. Jordan Brooks.	ICP-MS	<80	2.5±0.9	2.6±1

81	Uncleaned photo-etched phosphor-bronze TPC grid wires from Newcut Inc. Base material is entry 79.	ICP-MS	<80	250±15	6600±40
82	Uncleaned photo-etched phosphor-bronze TPC grid wires from Vaga Industries Base material is entry 79.	ICP-MS	200±50	56±1	358±5
83	Cleaned photo-etched phosphor-bronze TPC grid wires from Vaga Industries. Base material is entry 79.	ICP-MS	<90	47±2	320±2
84	Uncleaned photo-etched phosphor-bronze APD spider contacts from Newcut Inc. Base material is entry 80.	ICP-MS	<60	77±8	3300±20
85	Cleaned photo-etched phosphor-bronze APD spiders from Newcut Inc. Base material is entry 80.	ICP-MS	<60	65±5	1700±10
86	Uncleaned photo-etched phosphor-bronze APD spiders from Vaga Industries. Base material is entry 80.	ICP-MS	<60	9±1	113±1
87	Cleaned photo-etched phosphor-bronze APD spider contacts from Vaga Industries. Base material is entry 80.	ICP-MS	<70	8±1	71±3
88	Uncleaned photo-etched phosphor-bronze APD spider contacts from Vaga Industries using selected chemicals. Base material is entry 80.	ICP-MS	-	23±3	317±25
89	Cleaned photo-etched phosphor-bronze APD spider contacts from Vaga Industries using selected chemicals. Base material is entry 80.	ICP-MS	-	10.6±2.0	12.4±2.1
90	RD Chemical Company RD38, Vaga Industries photo-etch chemical.	A.G. Ge	<124000	<74000	-
91	DI water for Vaga Industries photo-etch.	A.G. Ge	<57000	<27000	<9200
92	Solid soda ash from Hill Brothers Inc., Vaga Industries photo-etch chemical.	A.G. Ge	<13200	<52000	39300±11300
93	Used ferric chloride from Phibro Tech Inc., Vaga Industries photo-etch chemical.	A.G. Ge	26100±7300	63200±7900	20300±2700
94	Fresh ferric chloride from Phibro Tech Inc., Vaga Industries photo-etch chemical.	A.G. Ge	<29000	<12300	<3300
95	RD Chemical Company RD87, Vaga Industries photo-etch chemical.	A.G. Ge	<54000	<89000	-
96	Alcohol, Vaga Industries photo-etch chemical.	A.G. Ge	<49000	<34000	<10100
97	California Fine Wire, 20 mil phosphor-bronze wire, annealed. Lot #24987.	GD-MS	<23	<20	<20
98	California Fine Wire, 20 mil Copper wire, annealed CFW-100-156 Lot #25477. <sup>60</sup> Co: <0.28 mBq/kg.	Ge	<180	<86	101±35
99	California Fine Wire, 20 mil annealed Cu wire, CFW-100-156, Lot #25477.	Shiva Inc., GD-MS	<0.5	<10	<10



100	California Fine Wire, 20 mil annealed Cu-Be wire, alloy 25, CFW-100-034.	Shiva Inc., GD-MS	<0.5	370000	1800000
-----	--	----------------------	------	--------	---------

**Photo-Etching: Cu on Polyimide Substrate**

101	Cu coating Nippon Steel Chemical Co., Espanex flat cable MC18-50-00CEM. Polyimide thickness: 50 $\mu\text{m}$ , Cu thickness: 18 $\mu\text{m}$ .	ICP-MS	-	<3 ( $<0.05 \text{ pg/cm}^2$ )	19 $\pm$ 2 ( $0.30\pm 0.03 \text{ pg/cm}^2$ )
102	Polyimide substrate Nippon Steel Chemical Co., Espanex flat cable MC18-25-00 CEM, lot 65605-11R1. Polyimide thickness: 25 $\mu\text{m}$ , Cu thickness: 18 $\mu\text{m}$ .	NAA*	<299	<1600	<1500
103	Cu coating Nippon Steel Chemical Co., Espanex flat cable MC18-25-00 CEM, lot 65605-11R1.	ICP-MS	-	69 $\pm$ 3 ( $1.1\pm 0.05 \text{ pg/cm}^2$ )	100 $\pm$ 3 ( $1.6\pm 0.04 \text{ pg/cm}^2$ )
104	Polyimide substrate, Nippon Steel Chemical Co., Espanex flat cable, MC15-40-00 VEG. Polyimide thickness: 40 $\mu\text{m}$ , Cu thickness: 15 $\mu\text{m}$ .	NAA*	107 $\pm$ 12	<450	<900
105	Cu coating, Nippon Steel Chemical Co., Espanex flat cable MC15-40-00 VEG.	ICP-MS	-	135 $\pm$ 6 ( $1.8\pm 0.07 \text{ pg/cm}^2$ )	67 $\pm$ 5 ( $0.9\pm 0.06 \text{ pg/cm}^2$ )
106	Nippon Steel Chemical Co., Espanex flat cable MC15-40-00VEG. $^{60}\text{Co}$ : <0.18 mBq/kg.	Ge	880 $\pm$ 120	<250	121 $\pm$ 32
107	Nippon Steel Chemical Co., Espanex flat cable MC18-25-00CEM, lot G5L03-23L2. $^{60}\text{Co}$ : <0.6 mBq/kg, $^{137}\text{Cs}$ : <1.3 mBq/kg.	Ge	<146	<260	<46
108	Polyimide substrate, Nippon Steel Chemical Co., Espanex flat cable MC18-25-00CEM, lot G5C03 23L2.	ICP-MS	390 $\pm$ 110 ( $1.4\pm 0.4 \text{ ng/cm}^2$ )	50 $\pm$ 17 ( $0.54\pm 0.06 \text{ pg/cm}^2$ )	450 $\pm$ 170 ( $1.6\pm 0.6 \text{ pg/cm}^2$ )
109	Cu coating, Nippon Steel Chemical Co., Espanex flat cable MC18-25-00CEM, lot G5C03 23L2.	ICP-MS	94 $\pm$ 19 ( $1.5\pm 0.3 \text{ ng/cm}^2$ )	34 $\pm$ 6 ( $0.55\pm 0.09 \text{ pg/cm}^2$ )	41 $\pm$ 6 ( $0.66\pm 0.1 \text{ pg/cm}^2$ )
110	Nippon Steel, Espanex flat cable, MC15-40-00 VEG. Etched by Basic Electronics. $^{60}\text{Co}$ : <0.56 mBq/kg, $^{137}\text{Cs}$ : <0.63 mBq/kg.	Ge	<160	<40	<97
111	Polyimide substrate Nippon Steel Espanex flat cable MC15-40-00 VEG. Etched Basic by Electronics.	ICP-MS	229 $\pm$ 71 ( $1.3\pm 0.4 \text{ ng/cm}^2$ )	317 $\pm$ 4 ( $1.8\pm 0.02 \text{ pg/cm}^2$ )	3880 $\pm$ 120 ( $22\pm 0.7 \text{ pg/cm}^2$ )
112	Cu coating Nippon Steel Espanex flat cable, MC15-40-00 VEG. Etched by Basic Electronics.	ICP-MS	105 $\pm$ 23 ( $1.4\pm 0.3 \text{ ng/cm}^2$ )	45 $\pm$ 4 ( $0.6\pm 0.05 \text{ pg/cm}^2$ )	1720 $\pm$ 23 ( $23\pm 0.3 \text{ pg/cm}^2$ )

**Avalanche Photo Diodes (Including Contact Metals)**

113	White sand used by Advanced Photonix for die cutting or beveling APDs <sup>5</sup> .	A.G. Ge	<38	58000±4500	45300±1800
114	Brown sand used for die cutting or beveling APDs.	A.G. Ge	720000±190000	(5.88±0.08)·10 <sup>7</sup>	(1.38±0.02)·10 <sup>7</sup>
115	Hydro Aluminium Deutschland, GmbH 6N Al for APD fabrication, ID B06HP054.	ICP-MS	170±40	45±2	44±2
116	Pechiney Al for APDs. Extended cleaning.	NAA	<460	<195	<560
117	Pechiney Al for APDs. Extended cleaning.	ICP-MS	170±60	33±2	49±2
118	Pechiney Al for APDs. Production cleaning only.	ICP-MS	190±40	38±6	76±4
119	Pechiney Al for APDs contact, no batch ID available.	GD-MS	<100	<50	<50
120	Pechiney Al for APDs.	Ge	490±160	<630	<360
121	Materials Research Corporation (MRC) Al for APDs, 20-101E-AL000-1000, purity grade 99.9995%.	GD-MS	<50	42000	6000
122	MRC Al for APDs 20-101E-AL000-1000, purity grade 99.9995%.	Shiva Inc., GD-MS	<5	29000	4100
123	MRC Al for APDs 20-101E-AL000-1000, purity grade 99.9995%.	NAA	<68000	48000±4800	5500±580
124	Ti for APD metallization.	GD-MS	<200	<100	<100
125	Pt for APD metallization.	ICP-MS	-	32±2	241±4
126	Au for APD metallization.	ICP-MS	-	612±18	79±2
127	Acid dissolved metal coating of Au contacted APD.	ICP-MS	-	6200±560	4500±280
128	APD pre-production ring wafer, supplier B. Orientation 1,1,1. Production cleaning only.	NAA*	<0.9	98±10	13.9±2.5
129	APD ring wafer, supplier A.	NAA	3.6±1	<1.8	<3.3
130	APD epi wafer.	NAA	<7.9	<4.9	<4.9
131	APD with Al contact. SN:155-B489 Al. Made using MRC Al.	NAA	30±6	70±8	<38
132	APD with Al contact. SN: 155-10-019 Al. Made using MRC Al.	NAA	22±4	101±11	<24
133	APD with Au contact, made using MRC Al.	NAA		<560	

<sup>5</sup> All APDs listed in this table were produced by Advanced Photonix, Inc.

134	APD with Au contact, made using MRC Al.	Alpha counting <sup>6</sup>	-	<220	<73
-----	---	-----------------------------	---	------	-----

#### Heat Transfer Fluids and Related Hardware

135	Cryogenic fluid 3M HFE-7000, lot 20016.	NAA*	<1.08	<7.3	<6.2
136	Cryogenic fluid 3M HFE-7000, lot: 20016, after exposing to Wessington dewar.	NAA*	<1.78	<2.8	<3.3
137	Cryogenic fluid 3M HFE-7000 lot 20018.	NAA*	<0.59	<8.4	<3.4
138	Cryogenic fluid 3M HFE-7000, lot 920001.	NAA	<0.58	<3.7	<7.3
139	Cryogenic fluid 3M HFE-7000, lot 20014. See Section 6 for analysis assumptions.	concentration + NAA*	-	<0.015	<0.015
140	Cryogenic fluid 3M FC-87.	NAA	<0.11	<0.95	<2.7
141	Cryogenic fluid 3M HFE-7100.	NAA	<0.21	<1.2	<2.1
142	Cryogenic fluid 3M HFE-7100.	NAA	<0.27	<3.4	<1.6
143	Silicon carbide. HFE pump thrust bearing material.	A.G. Ge	<65000	139000±39000	<44000
144	Tungsten carbide. HFE pump shaft material.	A.G. Ge	<42000	<42000	<20000

#### Miscellaneous Items

145	JL Goslar Pb free soldering wire, Esold EN ISO 12224-1/SN99, 3CuO, 7/1.1, type B1.	ICP-MS	-	<1	6570±280
146	Fluka p-terphenyl 99% purity.	NAA	72±7	25±3	0.5±0.6
147	Macor insulators.	A.G. Ge	<680000	359000±41000	528000±4000
148	Dow Corning ultra high vacuum grease.	A.G. Ge	<323000	<349000	116000±28000
149	Translucent platinum-cured silicone rubber o-rings from Simolex. Compound #: SIM4768Pt, supplier #: 4105/60 (Elastosil).	Balazs Analytical Services, ICP-MS	640(sample A) and 950(sample B)	<10000	<10000

<sup>6</sup> APD alpha counting was performed using the APD as both the sample and the detector, and is only sensitive to alphas from the active volume of the APD.

150	Transparent silicone-rubber o-rings from Perlast. Trans vmq 70-80 Plat Cured FDA/WRCC/USP class 6 grade, Compound # S80U, batch P6976.	Balazs Analytical Services, ICP-MS	790	<10000	<10000
151	Transparent silicone-rubber o-rings from Perlast. Trans vmq 70-80 Plat Cured FDA/WRCC/USP class 6 grade, Compound No. S80U, batch P6820.	Balazs Analytical Services, ICP-MS	1900	<10000	<10000
152	Transparent silicone-rubber o-rings from Perlast. Trans vmq 70-80 Plat Cured FDA/WRCC/USP class 6 grade, Compound No. S80U, batch P6820.	Ge	<19200	<47000	<7700
153	80 Buna-N Grottenrath Rubber Products Inc. o-rings of different sizes. Factor of 5 systematic uncertainty.	A.G. Ge	26±3.5	23400±1200	21700±340
154	Viton O-ring seal, Johannsen AG. <sup>60</sup> Co: <4.2 mBq/kg.	Ge	70000±7300	32000–54000	70000±7000
155	Sapphire window from Swiss Jewel Company, substrate for EXO high voltage resistors. EXO sapphire lot 2.	NAA*	<6.8	30±7	<25
156	Sapphire window from Swiss Jewel Company, substrate for EXO high voltage resistors. EXO sapphire lot 1.	Shiva Inc., GD-MS	<500	<10000	<10000
157	DuPont resistor paste 1108.	Ge	5400±1300	<4200	11500±1800
158	DuPont 6160 conductive paste.	Ge	43300±5700	<7500	5240±770
159	Resistive and conductive coating dissolved off EXO-200 sapphire-based field shaping resistors.	ICP-MS	<820	<3000	<2500
160	Un-encapsulated electro-optical level sensors, Gems Sensors, Series ELS-900, P/N 2007200.	Ge	101000±14000	335000±66000	153000±21000
161	Encapsulated electro-optical level sensors, Gems Sensors, Series ELS-900, P/N 2007200.	Ge	34000±3400	80000±16000	22000±3400
162	Si screw, Si: Wacker Chemie, machining: Holm Siliciumbearbeitung.	NAA	1.7±0.3	<1.2	<1.0
163	TSMC 0.25 μm process IC chip.	NAA	400±300	<151	<3200
164	CuSn6 phosphor-bronze 6%. 3/4 hard, 0.8 mm thick.	ICP-MS	<60	40±4	88±4
165	CuSn6 phosphor-bronze 6%. 3/4 hard, 0.8 mm thick. <sup>60</sup> Co: <0.60 mBq/kg, <sup>137</sup> Cs: 4.38±0.53 mBq/kg.	Ge	<360	<77	<170
166	CuSn6 phosphor-bronze 6%. 1/2 hard, 0.8 mm thick for cryostat door seal.	ICP-MS	110±40	50±3	78±4
167	CuSn6 phosphor-bronze 6%. 1/2 hard, 0.8 mm thick. <sup>60</sup> Co: <0.4 mBq/kg, <sup>137</sup> Cs: <1.6 mBq/kg.	Ge	<320	<81	<136

168	1/2" 544 phosphor-bronze rod.	ICP-MS	<20	15.9±2.6	18.6±2.3
169	1/4" phosphor-bronze washer. McMaster Carr #93490A029.	ICP-MS	-	36±4	43±9
170	1/4" 20×1" phosphor-bronze bolt. McMaster Carr #93516A542.	ICP-MS	188±13	38±4	43±3
171	Belleville washers, phosphor-bronze, SOLON 8L80 PB. <sup>60</sup> Co: <0.55 mBq/kg.	Ge	<280	1580±260	1240±140
172	Phosphor-bronze 544 for springs.	Shiva Inc. GD-MS	<10	60	40
173	Silicon-bronze 651 for springs.	Shiva Inc. GD-MS	<10	<5	<5
174	1/4" 655 silicon-bronze rod from Sequoia Brass and Copper.	ICP-MS	-	6.2±1.7	24.7±3.2
175	1/4" rod of 655 silicon-bronze from National Bronze and Metals Inc.	ICP-MS	97±11	<4.7	<3.1
176	1/4"-20×3/4" silicon-bronze screws. McMaster Carr #93516A540.	ICP-MS	182±15	<3.6	<3.9
177	1/2" silicon-bronze lock washer. McMaster Carr #93496A433.	ICP-MS	139±14	7.7±2.4	<4.2
178	5/8"-11 × 2" silicon-bronze screws. McMaster Carr #93516A752.	ICP-MS	<50	72±8	83±6
179	5/8" silicon-bronze lock washer. McMaster Carr #93496A435.	ICP-MS	<60	24±2	30±3
180	5/8" silicon-bronze washer. McMaster Carr #93490A035.	ICP-MS	<60	50±4	43±5
181	1/2"-13 × 2" hex head screws, C65100 Si-bronze. <sup>60</sup> Co: <0.46 mBq/kg.	Ge	<620	<490	213±51
182	Silicon-bronze screws and washers. <sup>60</sup> Co: <0.62 mBq/kg, <sup>137</sup> Cs: <0.70 mBq/kg	Ge	<250	<880	<120
183	Cu plus PET washers. <sup>137</sup> Cs: <10.7±1.8 mBq/kg.	Ge	<1040	<2800	2400±350
184	Swagelok 1" copper gasket CU-1-16-RP-2	ICP-MS	229±16	9.1±1.7	20.4±2.5
185	Swagelok 1" brass fitting 1610-1-16RS.	ICP-MS	<19	8.2±2	27.4±2.4
186	Swagelok 1/2" brass fitting B-810-1-12, machined to custom shape.	ICP-MS	-	12.5±1.4	12.4±1.3
187	Swagelok 1/2" brass fitting B-810-1-12, extra cleaning, machined to custom shape.	ICP-MS	-	5.1±0.7	7.9±0.7
188	Swagelok ferrules for brass fitting B-810-1-12, second shipment. Machined to custom shape.	ICP-MS	<28	12±1	10.0±0.8
189	Swagelok body for brass fitting B-810-1-12, second shipment. Machined to custom shape.	ICP-MS	<35	<2.7	<1.7
190	1/2" copper gasket, Serto #SO 40007-18.	ICP-MS	260±31	6.9±2.5	12.6±2.2
191	1/2" copper gasket, Serto #SO 40007-18. Second shipment.	ICP-MS	-	7.5±3.5	10.2±2.8

192	1/2" Indium plated (New Brunswick Plating) Serto copper gasket. Un-plated gasket is item 190.	ICP-MS	189±22	7.5±1.3	19.2±2.4
193	Indium plated (New Brunswick Plating) Jetseal phosphor-bronze gasket. phosphor-bronze is item 166.	ICP-MS	-	66.9±6.0	78.2±9.7
194	1" Indium plated (New Brunswick Plating) copper gasket. Un-plated gasket is item 184.	ICP-MS	146±14	14.5±1.5	27.5±3.1
195	Helicoil Stainless Steel, various sizes (194 × 1/2-13 1185-8CN500 190 × 1/4-20 1185-4CN375 96 × 3/4-20 1185-12CN750 190 × 8-32 1185-2CN328). <sup>60</sup> Co: 41±2 mBq/kg.	Ge	<430	<320	<193
196	10 gauge copper wire, McMaster-Carr, ID 7512 K552. <sup>60</sup> Co: <0.23 mBq/kg, <sup>137</sup> Cs: <1.5 mBq/kg.	Ge	1190±250	<77	<270
197	10 gauge copper wire, McMaster-Carr, ID 7512 K552.	ICP-MS	-	30±2	11±1
198	10 gauge copper wire, McMaster-Carr, ID 7512 K552. Second purchase.	ICP-MS	<60	29±2	16±1
199	Polyethylene insulator from Consolidated Wire and Cable RG217 coax high voltage cable.	NAA	47±7	<140	<240
200	Copper wire from Consolidated Wire and Cable RG217 coax high voltage cable.	ICP-MS	118±17	4.4±2.6	6.0±2.5
201	Polyethylene insulator from Pasternack RG217 coax high voltage cable.	NAA	129±17	<360	355±107
202	Copper wire from Pasternack RG217 coax high voltage cable.	ICP-MS	105±15	<4.7	4.1±2.3
203	20 gauge silicone rubber high voltage cable from Able Wire Company. <sup>60</sup> Co: <0.62 mBq/kg, <sup>137</sup> Cs: <0.71 mBq/kg.	Ge	19200±2100	36400±3700	34600±3500
204	Two component urethane potting mixture, Epoxies Etc. Resin 20-2350R CLR, catalyst 20-2350C, 100:7.5 mix.	NAA*	11.4±2.2	<37	<94
205	Two component epoxy, Epoxies Etc. Resin 20-3001R clear, catalyst 20-3001C, 1:1 mix.	NAA*	<20	<23	<44
206	Two component low temperature silicone rubber. Component A GE-RTV567A product# 009454, component B GE-RTV567B, product# 38014, 15:1 mix.	NAA*	(14.4 ± 1.4) · 10 <sup>6</sup>	-	237±59
207	Epon 828 epoxy resin, manufactured by Hexion. <sup>60</sup> Co: <0.5 mBq/kg, <sup>137</sup> Cs: <0.5 mBq/kg	Ge	<200	<150	<250
208	14 m 1/4" OD, 1/6" ID PTFE tubing, McMaster-Carr # 5033 K316. <sup>60</sup> Co: <5.8 mBq/kg, <sup>137</sup> Cs: <10.8 mBq/kg.	Ge	<6400	<700	<2900
209	3/16" Copper tubing. Wolverine Tube Inc. McMaster Carr # 5174 K2, Cu alloy 122.	ICP-MS	<60	74±4	<1

210	1/2" Cu tubing for heat exchangers. Metallica SA.	ICP-MS	-	<2	<1.5
211	1/2" Cu tubing for heat exchangers. Metallica SA.	Ge	<180	<790	<113
212	1" Cu tubing for HFE. McMaster-Carr, Cu-alloy 122.	ICP-MS	<27	40±2	<1.5
213	Closed cell PE foam, Uline 1/8" × 72 in × 550'. <sup>60</sup> Co: <23 mBq/kg, <sup>137</sup> Cs: <29 mBq/kg.	Ge	<14800	<19200	32000±4600
214	Closed cell PE foam, Pacific States Felt & Mfg. Co. Inc., 1/8" thick	NAA <sup>a</sup>	7820±960	14000±4000	<4900
215	Omega Engineering Inc. thermocouple, part TT-T-30-SL. <sup>60</sup> Co: <8.0 mBq/kg.	Ge	<7000	<3800	<1700
216	Polyimide tape from Stanford stock room.	A.G. Ge	<37000	<5400	<5800
217	Sheldal superinsulation, item # 146477, 0.25 mil PET aluminized on one side.	Ge	5550±1300 (4.9±1.2 ng/cm <sup>2</sup> )	<4080 (<3.7 pg/cm <sup>2</sup> )	4660±380 (4.1±0.4 pg/cm <sup>2</sup> )
218	Sheldal superinsulation, item # 146477, 0.25 mil PET aluminized on one side. K result is for dissolved aluminum layer only but normalized to whole sample mass. For U and Th, the PET layer was also partially dissolved and analyzed.	ICP-MS	461±33 (0.41±0.03 ng/cm <sup>2</sup> )	<1800 (<1.6 pg/cm <sup>2</sup> )	5740±150 (5.1±1.3 pg/cm <sup>2</sup> )
219	Sheldal superinsulation, item # 146455, 0.3 mil DuPont Kapton aluminized on one side.	ICP-MS	-	<1640 (<1.75 pg/cm <sup>2</sup> )	<6100 (<6.5 pg/cm <sup>2</sup> )
220	Sheldal superinsulation, item # 146428, 0.3 mil DuPont Kapton aluminized on both sides, embossed.	ICP-MS	-	<1540 (<1.64 pg/cm <sup>2</sup> )	2500±800 (2.64±0.85 pg/cm <sup>2</sup> )
221	Jehier candidate superinsulation mix for EXO before installation: 26 layers of Insulray 305 plus 4 layers of Teril-53. <sup>60</sup> Co: <3.8 mBq/kg.	Ge	<6500	<4100	7700±1000
222	Jehier superinsulation mix sampled after installation without further cleaning.	NAA	51400±2100	<13900	12300±5540
223	Plastic and metallization of Jehier superinsulation EXO-mix.	ICP-MS	-	<80	<60
224	Jehier superinsulation, EXO-mix. Second purchase. <sup>60</sup> Co: <16 mBq/kg, <sup>137</sup> Cs: <16 mBq/kg.	Ge	18600±5000	<1700	3900±1300
225	Jehier hook-and-loop fastener to hold superinsulation.	Ge	3090±890	<1670	<920

## References

- [1] M. Danilov, et al., *Phys. Lett. B* 480 (2000) 12; M. Breidenbach, et al., Letter of intent to SLAC EPAC, LOI-2001.1, August 2001, unpublished.
- [2] F. LePort, A. Pocar, et al., *Nucl. Instr. and Meth. A* 578 (2007) 407.
- [3] M. Redshaw, et al., *Phys. Rev. Lett.* 98 (2007) 053003.
- [4] E.-I. Esch, et al., *Nucl. Instr. and Meth. A* 538 (2005) 516.
- [5] C. L. Chou, J. D. Moffatt, *Fresenius Journal of Analytical Chemistry* 368 (2000) 59.
- [6] A. E. Eroglu, C. W. McLeod, K. S. Leonard, D. McCubbin, *Spectrochimica Acta Part B Atomic Spectroscopy* 53 (1998) 1221.
- [7] J. C. Lozano, F. Fernandez, J. M. G. Gomez, *Appl. Radiat. Isot.* 50 (1999) 475.
- [8] J. S. Becker, H. J. Dietze, *J. Anal. At. Spectrom.* 13 (1998) 1057.
- [9] J. S. Becker, W. Kerl, H. J. Dietze, *Anal. Chim. Acta* 387 (1999) 145.
- [10] K. Tagami, S. Uchida, *J. Radioanal. Nucl. Chem.* 197 (1995) 409.
- [11] S. Vijayalakshmi, R. K. Prabhu, T. R. Mahalingam, C. K. Mathews, *Atomic Spectroscopy* 13 (1992) 61.
- [12] H. E. Carter, P. Warwick, J. Cobb, G. Longworth, *Analyst* 124 (1999) 271.
- [13] J. Chai, Y. Oura, M. Ebihara, *J. Radioanal. Nucl. Chem.* 255 (2003) 471.
- [14] A. P. Mykytiuk, P. Semeniuk, S. Berman, *Spectrochimica Acta Review* 13 (1990) 1.
- [15] M. R. Winchester, R. Payling, *Spectrochimica Acta Part B Atomic Spectroscopy* 59 (2004) 607.
- [16] P. Grinberg, S. Willie, R. E. Sturgeon, *Analytical Chemistry* 77 (2005) 2432.
- [17] Z. Djurcic, D. Glasgow, L.-W. Hu, R. McKeown, A. Piepke, R. Swinney, B. Tipton, *Nucl. Instr. and Meth. A* 507 (2003) 680.
- [18] D. Arnold, private communication (2003).
- [19] J. Boger, et al., *Nucl. Instr. and Meth. A* 449 (2000) 172.